

Article Title

Bridge damage detection using weigh-in-motion technology

Authors

Daniel Cantero

Arturo González

Manuscript version

Post-print = Final draft post-refereeing, before copy-editing by journal

DOI:

[10.1061/\(ASCE\)BE.1943-5592.0000674](https://doi.org/10.1061/(ASCE)BE.1943-5592.0000674)

Reference:

Cantero, D., González, A., (2017). Bridge damage detection using weigh-in-motion technology. *ASCE Journal of Bridge Engineering*, Volume 20, Issue 5, May 2017.

Post-Print

Title:

Bridge damage detection using weigh-in-motion technology

Authors:

Daniel Cantero¹ and Arturo González²

1) Roughan & O'Donovan Innovative Solutions, Arena House, Arena Road, Sandyford, Dublin 18, Ireland. Tel: 00353 834 6731; Email: canterolauer@gmail.com;

2) School of Structural, Civil and Environmental Engineering, University College Dublin, Dublin 4, Ireland

Abstract:

This paper proposes a novel level I damage detection technique for short to medium span road bridges using weigh-in-motion (WIM) technology. The technique is based on the input provided by two different WIM systems: (a) a pavement-based WIM station located in the same route as the bridge (which gives vehicle weight estimates without the influence of the bridge) and (b) a bridge-based WIM system which estimates vehicle weights based on the deformation of the bridge. It is shown that the ratio of estimations of vehicle weights by both systems is a reliable and robust indicator of structural integrity even for WIM systems with relatively poor accuracy. Furthermore, this indicator is shown to be more sensitive to damage than the traditional method based on variation in natural frequencies.

Keywords:

Weigh-in-Motion, bridge, damage detection, local and global damage, structural health monitoring

Introduction

Road network owners have to manage an ever growing infrastructure stock for steadily increasing traffic volumes. Thus, a significant part of the available budget is spent on maintenance and reparation works. This has been reflected in research, where the interest in structural health monitoring (SHM) and assessment has surpassed the contributions in structural design. There is no single solution for the correct monitoring and assessment of the infrastructure due to the variety of structures, materials, loads and environmental conditions to consider for a particular site. Therefore, a combination of damage assessment technologies is necessary and new SHM developments aim to cover as many structures as possible within a reasonable cost.

While a majority of bridges are assessed via periodical visual inspections, they are expensive, scattered in time and prone to error, and vibration-based SHM techniques are emerging, mainly on large newly-built bridges. There are many possible ways to define a SHM system, the number of sensors, type and their location. For example, Level I damage identification methods (Doebbling 1998) intend to detect the presence of damage in the structure and require relatively simple installations, but they are not able to either locate (Level II) or quantify damage (Level III), or predict the remaining service life of the structure (Level IV). Level I methods generally provide an easy and quick way of monitoring structural changes which could lead to further action when those changes exceeded an established threshold; i.e., through the application of higher (and typically more sophisticated and costly) levels of damage detection. The most popular level I damage identification methods using vibrations due to traffic are based on frequencies and modes to be extracted from sensors installed at

various locations on the bridge. Changes over time in natural frequencies and mode shapes could denote structural deterioration (Gomez et al. 2011). However, natural frequencies change only slightly for significant damage and it is not always clear if changes are due to factors other than damage, i.e., environmental.

This paper proposes a new level I damage identification method for short to medium span bridges by using the combined information of two Weigh-in-Motion (WIM) systems. WIM systems comprehend a wide range of technologies that allow estimating wheel weights and axle spacing of road vehicles moving at full speed and can be categorized as pavement-based or bridge-based technologies.

Pavement-based WIM systems are located on the road surface or embedded in the pavement generating the signals that after some manipulation will provide the desired traffic information, namely axle weights, spacing and speed. Given that the WIM sensor is only able to weigh the axle for a very short period of time, the accuracy in the estimation of traffic weights is clearly affected by the oscillating nature of the applied axle load and noise. This accuracy will vary with the quality of the weighing sensor, the number and spacing of sensors, and the unevenness of the road profile. There are different types of WIM sensors available in the market including piezos, pressure cells, bending plates and inductive loops, among others. Since its appearance in the 1950's, sensitivity and accuracy have largely been enhanced and WIM is nowadays a technology used worldwide.

Bridge-based WIM (B-WIM) systems record the deformation of the bridge (typically strains) while the vehicle of interest is traversing the structure and use this information to estimate the vehicle's weight distribution. The first and most popular B-WIM algorithm to calculate vehicle weights was introduced by Moses (1979) and searches for the weight distribution that best fits the recorded response based on the structure's influence line of strain at each gauge location. During the installation of the B-WIM system, the structure's influence line is calibrated on-site using a vehicle of known speed, axle spacing and weights (OBrien et al. 2006). In addition to noise and inaccuracies associated to the sensors, their resolution and installation, typical sources of error for B-WIM systems are related to the difficulty in: (a) separating the static response from the measured total response (this separation is more difficult the longer and more flexible the bridge. For this reason, long span bridges are not suitable for B-WIM purposes), (b) identifying the contribution of closely spaced individual axles, (c) locating the vehicle precisely on the bridge at each point in time, and (d) obtaining an accurate influence line on site. B-WIM systems tend to predict Gross Vehicle Weights (GVWs) more accurately than individual axle weights (McNulty and OBrien 2003) and are particularly suited for stiff short straight spans (i.e., culverts or integral bridges) (González 2010).

Data gathered by WIM systems have covered many applications, including pavement and bridge design, assessment and monitoring (i.e., using WIM data to produce a more accurate picture of the traffic load model that the infrastructure must be designed/assessed for (O'Connor and OBrien 2005, Wilson et al. 2006), or to monitor loads for fatigue calculations (Wang et al. 2005)), management of road infrastructure (i.e., to decide on road maintenance strategies), traffic planning and weight enforcement (i.e. to protect the infrastructure, ensure safety and a fair competition between network users (Han et al. 2012)). B-WIM has also been used as a form of soft load testing, where experimental influence lines (OBrien et al. 2008) and dynamic measurements (Žnidarič et al. 2008) have been obtained. However, to the authors' knowledge direct WIM outputs have not been specifically used for damage

identification yet. By using one pavement-based WIM system installed near the bridge (leading to first GVW estimations of the traffic) and a B-WIM system in the bridge under investigation (providing second GVW estimations of the same vehicles), it is possible to propose a method that will identify the occurrence of bridge damage in time.

The implementation of the proposed damage identification technique would require instrumenting every bridge to be monitored with a B-WIM system. B-WIM systems are typically more economical than pavement-based WIM, mobile and its installation does not interfere with the traffic since the sensors are located under the bridge soffit. Although the competition in the WIM market has led to a reduction in costs, pavement-based WIM remains expensive, its installation produces disruption of the traffic and needs periodic maintenance and recalibration as its sensors are subject to adverse conditions and repetitive heavy loads. However, the number of pavement-based WIM stations can be significantly smaller than B-WIM systems if an efficient monitoring strategy is devised, i.e., by allocating one WIM station on a route through multiple bridges under surveillance. The axle weight estimates from the WIM can be correlated with the estimates from the B-WIM assuming a meaningful proportion of heavy vehicles will cross and be identifiable in both systems. In the case of an instrumented bridge where the pavement-based WIM system is not installed just before or after the bridge, there will be some traffic scenarios such as road congestions that will delay the arrival of the vehicles, or even worse, some vehicles that might not reach the pavement-based WIM or bridge because they left the road in an exit prior to them. The number of correlated vehicle events can be improved by including some sort of vehicle recognition technology before each bridge (i.e., video cameras). A future possibility is related to the growth of number of vehicles with built-in positioning systems, information that if made available to the network owners, it will facilitate the identification of the same vehicle in each WIM system in real-time. In any case, it is expected there will be periods of traffic that will facilitate to correlate a significant proportion of vehicles crossing both WIM systems for monitoring purposes (i.e., based on vehicle configuration, time of arrival, etc.). Figure 1 illustrates the proposed SHM concept, where the data from the WIM stations is sent to a common post-processor to be analyzed.

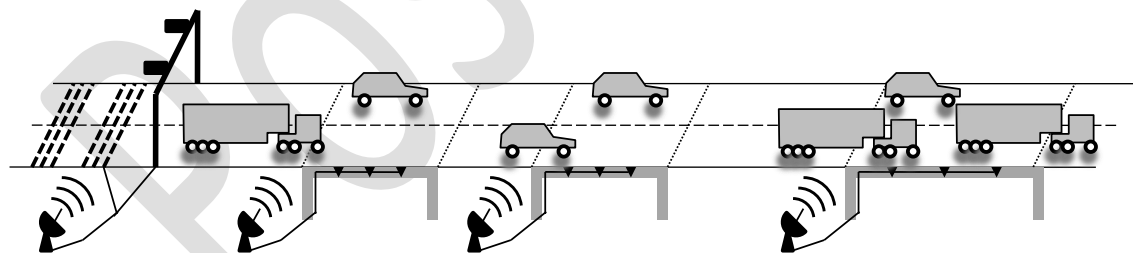


Figure 1. Weigh-In-Motion based damage identification concept for structural health monitoring of bridges.

The principle behind the WIM-based SHM method is that if the bridge suffers some local or global damage, the structure's response will change and as a result, the B-WIM system (calibrated on the basis of a different structural condition and influence line) will provide incorrect GVW estimations. In the following sections, it will be shown that the relative difference between vehicle weights estimations by B-WIM and pavement-based WIM systems can be used as an indicator of structural integrity. This indicator can be periodically updated with the continuous traffic data provided by WIM. In this paper, a numerical vehicle-bridge interaction simulation model is employed to compare the performance of the proposed damage indicator with that of a traditional Level I damage identification method based on

changes in natural frequencies. Finally, the versatility of the new damage detection technique to capture both global and local damage under adverse road conditions is tested for different levels of damage severity.

Theoretical basis

This section explains why the proposed method is able to successfully detect damage. The total static strain, defined at discrete time points j , at any particular section of the structure (typically mid-span) due to a moving vehicle can be calculated by adding the individual contribution of each axle weight to the static strain. This contribution is the result of multiplying the weight of each axle by the ordinate of the influence line of strain at the axle location for each point in time. This system of equations is expressed in matrix form in equation (1).

$$\{\varepsilon\} = [IL] \cdot \{A\} \quad (1)$$

where $\{\varepsilon\}$ is a vector containing the static strain of dimension $(T \times 1)$ being T the total number of sampling points; $\{A\}$ is a vector containing axle weights of dimension $(N \times 1)$ being N the total number of axles; and $[IL]$ is a matrix of dimension $(T \times N)$ composed of influence line ordinates which are function of the position of each axle at each point in time.

The measured strain $\{\varepsilon^m\}$ is not only made of a static component $\{\varepsilon\}$, but also a dynamic component. Given that the dynamic component oscillates about the static component, Moses proposes to find the weight of each axle by minimizing the difference between the measured response $\{\varepsilon^m\}$ and the theoretical static response $\{\varepsilon\}$. Equation (2) provides the error function given by the sum of the squared differences between measured ε_j^m and static strain ε_j (where ε_j are the components of the vector $\{\varepsilon\}$ obtained using equation (1)), for every point in time j .

$$\Psi = \sum_{j=1}^T (\varepsilon_j^m - \varepsilon_j)^2 \quad (2)$$

Minimizing the objective function Ψ with respect to A_i , it is possible to obtain equation (3). Full details can be found in Moses (1979).

$$\{A\} = [[IL]^T [IL]]^{-1} [IL]^T \{\varepsilon^m\} \quad (3)$$

The equation above remains to be the basis for B-WIM algorithms in commercial B-WIM systems.

When a B-WIM system is installed for the first time, it needs to be calibrated before becoming operational. The influence line is determined during the calibration process using trucks of known configuration and weight distribution driving over the bridge at typical traffic speeds. Once the influence line is known, the $[IL]$ matrix can be easily constructed for any truck configuration and speed, and the truck axle weights can be calculated via the measured strain $\{\varepsilon^m\}$ and the application of equation (3).

Over time, the structure might deteriorate changing the manner it responds to loads, i.e., resulting in an influence line $[\tilde{IL}]$ different to the one $[IL]$ obtained during calibration. Therefore, axle weights would ideally be calculated now using the equation (4):

$$\{\tilde{A}\} = \left[[\tilde{IL}]^T [\tilde{IL}] \right]^{-1} [\tilde{IL}]^T \{\varepsilon^m\} \quad (4)$$

where $\{\tilde{A}\}$ are the true axle weights traversing the current bridge (defined by a matrix of new influence line ordinates $[\tilde{IL}]$). However, the installed B-WIM system will inadvertently continue to estimate the axle weights with the information obtained during calibration, i.e., $[IL]$ and equation (3). For example, in the case of the same vehicle and measured strain, $\{\varepsilon^m\}$ can be cancelled out by combining equations (3) and (4), and then, the following relationship between estimated axle weights using original influence lines and current influence lines can be obtained:

$$\{\tilde{A}\} = \left[[\tilde{IL}]^T [\tilde{IL}] \right]^{-1} [\tilde{IL}]^T [IL]^{-1} \left[[IL]^T [IL] \right] \{A\} \quad (5)$$

In the equation above, if the influence line of the bridge has not changed, $[\tilde{IL}] = [IL]$ and $\{\tilde{A}\} = \{A\}$. However, if the influence line in the period between the two calculations is different, then $\{\tilde{A}\} \neq \{A\}$.

Equations (4) and (3) define the current load on the bridge $\{\tilde{A}\}$ and the B-WIM weight estimation $\{A\}$ respectively through products of old and new values of influence ordinates. Incorrect axle weight predictions $\{A\}$ by the B-WIM system with regards to the actual vehicle weight configuration $\{\tilde{A}\}$ will indicate changes in the structure's influence line. In the case that the structure has not suffered any changes, both influence lines are identical ($[IL] = [\tilde{IL}]$) and the B-WIM system will estimate the correct axle weight (equation (5)) except for sources of inaccuracy (i.e., dynamics, noise, inaccurate truck location) different from the influence line. It is clear that if both $\{A\}$ and $\{\tilde{A}\}$ were available, then their relationship could be potentially used for SHM. With this in mind, the authors propose the relative difference in GVW prediction (E_{BWIM}) defined in equation (6) as a new tool to monitor structural changes.

$$E_{BWIM} = \frac{\sum_{i=1}^N A_i - \sum_{i=1}^N \tilde{A}_i}{\sum_{i=1}^N \tilde{A}_i} \times 100 \quad (6)$$

where N is number of axles, A_i is the weight estimation of axle i by the B-WIM system, and \tilde{A}_i is the true weight of axle i , being the latter approximated by a pavement-based WIM system. The sensitivity of E_{BWIM} to damage is tested in subsequent sections, where significant

changes of E_{BWIM} over time will indicate that the influence line has changed and probably damage has occurred.

Simulation model

This section describes the numerical model used to simulate a vehicle traversing a beam. The bridge is represented by a finite element model discretized into 100 beam elements (each element being 0.1 m long) with properties presented in Table 1. Two types of boundary conditions have been considered in the paper, namely simply supported and fixed-fixed, and the first three natural frequencies associated to each bridge are listed in Table 2. Figure 2 shows a sketch of the beam and the location of the three B-WIM strain sensors employed in the simulations. Using various strain sensors along the beam span is common practice in modern non-intrusive B-WIM systems (O'Brien et al. 2008).

Table 1. Bridge model properties.

Description	Value
L Total span length (m)	10
ρ Mass per unit length (kg/m)	18750
E Young's modulus (N/m ²)	$3.5 \cdot 10^{10}$
I Section moment of inertia (m ⁴)	0.1609
ζ Damping (%)	3

Table 2. Natural frequencies of bridge models.

Boundary condition	Simply supported	Fixed-fixed
1 st frequency (Hz)	8.61	19.52
2 nd frequency (Hz)	34.44	53.80
3 rd frequency (Hz)	77.49	105.47

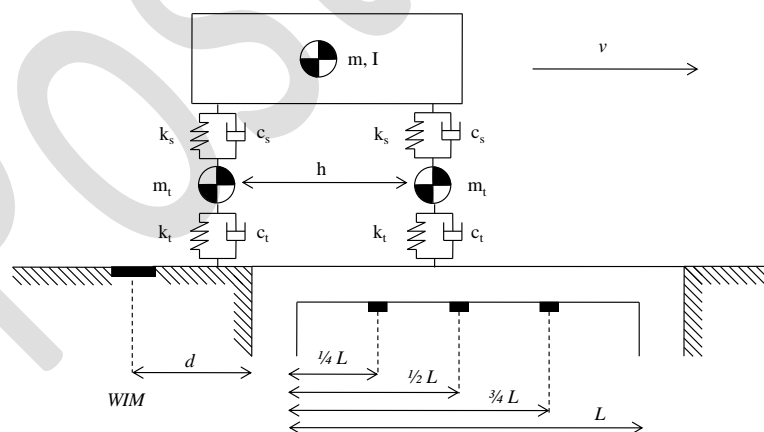


Figure 2. Vehicle and Bridge sketches with WIM and B-WIM sensor locations.

The vehicle model is a 4-DOF two-axle system as illustrated in Figure 2. The main body and tire masses are connected to each other and to the road profile by spring and dashpot systems. Vehicle properties are assumed to follow a normal distribution of mean and standard deviation defined in Table 3. Values are randomly sampled from these statistical distributions typical of two-axle trucks (which are bounded by the minimum and maximum values provided in the table to prevent unrealistic properties) using Monte Carlo simulation to generate traffic populations. Unless otherwise specified, the vehicle models will be simulated

running over a class ‘A’ road profile with a geometric spatial mean of $32 \cdot 10^{-6} \text{ m}^3$ (ISO 1995) of 100 m length before arriving to the bridge to allow for the system to reach dynamic equilibrium. Once on the structure, the equations of motion of vehicle and beam models are integrated and solved iteratively to obtain the response of the coupled system, i.e., vehicle forces and $\{\varepsilon^m\}$. Further details on the particularities of the models, the iterative solution and vehicle properties can be found in (Cantero et al. 2011). Equation (3) is then used to obtain the GVW solution by the B-WIM system from $\{\varepsilon^m\}$, and the value of the time-varying axle forces when they are located 2 m prior to the bridge are added together to simulate the GVW provided by a WIM system at that road section.

Table 3. Range of vehicle properties.

Property	Name	Unit	Average	Standard deviation	Minimum	Maximum
Body mass	m	kg	$10 \cdot 10^3$	$3 \cdot 10^3$	$5 \cdot 10^3$	$20 \cdot 10^3$
Body Moment of Inertia	I	$\text{kg} \cdot \text{m}^2$	$100 \cdot 10^3$	$20 \cdot 10^3$	$80 \cdot 10^3$	$200 \cdot 10^3$
Suspension Stiffness	k_s	N/m	$1 \cdot 10^6$	$0.3 \cdot 10^6$	$0.5 \cdot 10^6$	$2 \cdot 10^6$
Suspension damping	c_s	N·s/m	$10 \cdot 10^3$	$3 \cdot 10^3$	$5 \cdot 10^3$	$20 \cdot 10^3$
Tire mass	m_t	kg	$1 \cdot 10^3$	$0.5 \cdot 10^3$	$0.5 \cdot 10^3$	$2 \cdot 10^3$
Tire stiffness	k_t	N/m	$1 \cdot 10^6$	$0.3 \cdot 10^6$	$0.5 \cdot 10^6$	$2 \cdot 10^6$
Tire damping	c_t	N·s/m	$10 \cdot 10^3$	$3 \cdot 10^3$	$5 \cdot 10^3$	$20 \cdot 10^3$
Axle spacing	h	m	5	1	3	7
Velocity	v	km/h	80	20	50	120

Comparison of WIM-based and frequency-based SHM approaches

In this section the sensitivity of the proposed SHM concept to damage is directly compared to the theoretical variations in natural frequencies. Two types of structural damage are considered, namely global and local damages, which are treated separately. Here, global damage is modeled reducing the stiffness of all elements by a fixed percentage simultaneously. Local damage is modeled reducing the stiffness at only one particular element (0.1 m long) and its location and percentage of reduction is specified for each scenario.

Note that this section deals with an ideal and unrealistic situation of a single-axle vehicle where both pavement-based and B-WIM systems are able to calculate the applied static weights exactly, except for errors derived from changes in the influence line. This theoretical analysis facilitates to isolate errors in weight estimation due to a wrong influence line (due to a global or local stiffness reduction) from other sources of WIM inaccuracy such as dynamic oscillations around the static response due to the presence of a profile or the inherent vehicle-bridge interaction that will be considered later, in Section 5, with the use of a 4-DOF two-axle vehicle (Figure 2).

Global damage

Figure 3a shows the influence lines of the fixed-fixed beam at two particular sections in the case of global damage (20% global stiffness reduction). It shows that when global damage occurs, greater strains are observed on the beam due to its reduced stiffness (dashed line) with respect to a previous state (solid line). Similar trends can be observed on the simply

supported beam case (Figure 3b). Note that the strain influence lines presented in Figure 3 are normalized with respect to the maximum strain at mid-span. Using these influence lines together with equation (3), to calculate the weight of a single moving constant load, E_{BWIM} is 25% for any sensor location of the B-WIM along the beam. This means E_{BWIM} is amplifying the reduction in stiffness (which has been 20%). It must be noticed that for a global reduction in stiffness, E_{BWIM} will be positive, while for a global increase in stiffness (i.e., due to bridge strengthening or environmental factors), E_{BWIM} will be negative.

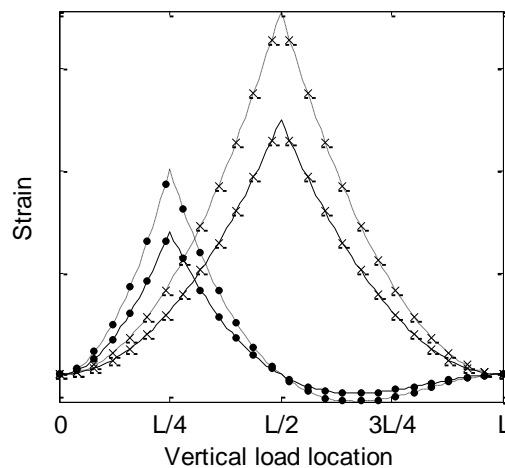


Figure 3. Strain influence line for sensors located at $1/4L$ (dots) and $1/2L$ (crosses); for healthy (solid lines) and 20% reduction of global stiffness (dashed lines).

Figure 4 shows the relative variation of the beam's natural frequencies compared against the variation of E_{BWIM} for a range of degrees of global damage. As mentioned earlier, stiffness reductions are reflected in increases of E_{BWIM} , whereas natural frequencies show a negative variation. For clarity and ease of comparison, the relative variations are presented in absolute values in Figure 4. This figure shows that for the same amount of global damage, the E_{BWIM} indicator approximately doubles the sensitivity to damage of a frequency-based approach. For instance, in the case of a simply supported bridge (Tables 1 and 2), when a 20% global stiffness reduction is considered, the fundamental frequency (8.61Hz) is reduced to 7.70Hz, which represents a 10.56% reduction, while E_{BWIM} reaches 25%.

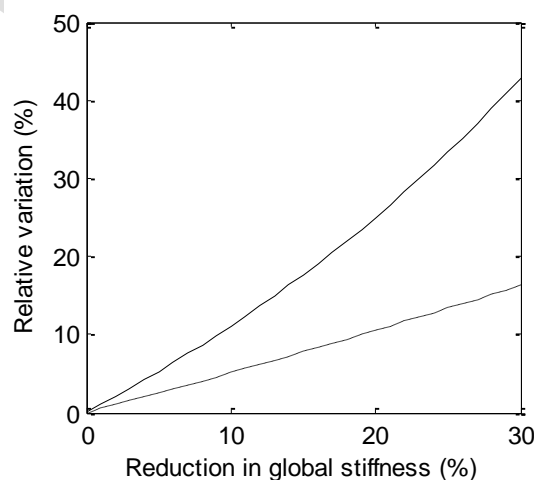


Figure 4. Relative changes in absolute value due to global damage for E_{BWIM} (solid) and natural frequency (dashed).

It is important to note that the same relative variations in natural frequencies are obtained for any of the natural frequencies under consideration and for any type of boundary condition. This can easily be explained from the well-known expression for the natural frequencies of a beam, presented in equation (7) (Yang 2005), where μ_k are the roots of the characteristic equation which depend only on the boundary conditions. Thus, global stiffness reductions of the beam lead to proportional frequency variations for any of the infinite number of frequencies.

$$f_k = \frac{1}{2\pi} \left(\frac{\mu_k}{L} \right)^2 \sqrt{\frac{EI}{\rho}} \quad (7)$$

Similarly, for a given change in global damage, E_{BWIM} is identical for any type of boundary condition. This can be explained because in this situation changes in influence lines are proportional to changes in global stiffness.

Local damage

Compared to global damage, the new influence lines of strain for a structure damaged locally do change only slightly, and only when the structure is statically indeterminate (For a statically determinate structure, localized changes in stiffness will not be noticeable in the influence line of strain unless the measurement location is at the damaged location). For the sake of a clear visualization, an unrealistic severe local damage (95% stiffness reduction) is modeled at the mid-span element of a fixed-fixed beam and the associated influence lines are shown in Figure 5.

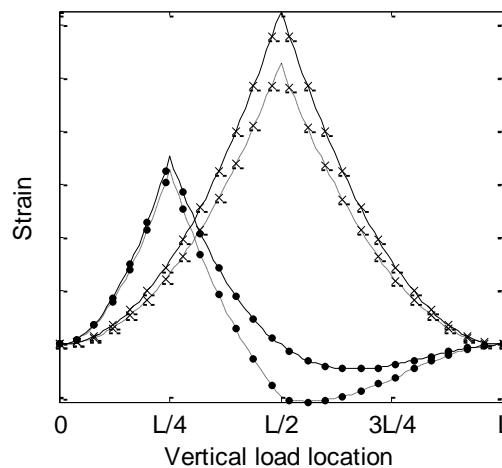


Figure 5. Strain influence line for sensors located at $\frac{1}{4}L$ (dots) and $\frac{1}{2}L$ (crosses); for healthy (solid lines) and 95% local damage at $\frac{1}{2}L$ (dashed lines).

In the case of local damage, sensitivity depends on the damage location, severity and bridge boundary conditions and it is more complex than the global damage case investigated in the previous sub-section. Figure 6(a) shows E_{BWIM} for three different strain sensor locations considering local damages of 50% stiffness reduction for different positions of the damaged element throughout the beam length. Figure 6(b) shows the relative variations in natural frequencies for the same damage scenarios. As for global damage, Figure 6 results are valid

for any span length if the chosen damage length ($L/100$) is equally proportional to the bridge span (L).

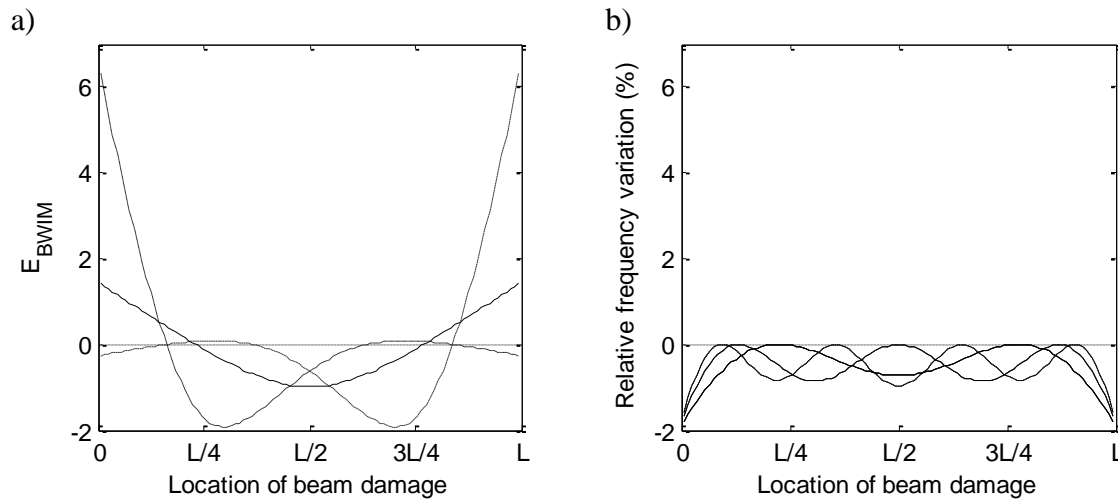


Figure 6. Influence of 50% local stiffness reduction for different positions of the damaged element on (a) E_{BWIM} for sensors located at $L/4$ (dashed); $L/2$ (solid); $3L/4$ (dash-dot); (b) Relative change in 1st (solid), 2nd (dashed) and 3rd (dash-dot) natural frequencies.

Damage indicators at a given measurement point feature zero values for particular damage locations. For instance, a local damage at $L/4$ will go unnoticed to E_{BWIM} for a sensor at mid-span or $3/4$ span, but can be captured by a sensor at $L/4$. Similarly, the 1st natural frequency would not be affected by a local damage at $L/4$ and no damage prediction would be possible without using higher frequencies. Thus, combinations of various sensors or the consideration of a few natural frequencies are necessary to be able to monitor local damages across the full beam length. Here lays one of the strengths of the proposed method: while it can become difficult to accurately measure high frequencies or relatively small frequency changes, strain records at different locations can provide robust and reliable E_{BWIM} values, typically more sensitive the closer the measurement and damage locations.

Additionally, Figure 6 shows that in general E_{BWIM} values are greater than the relative variation of natural frequencies. This can be explained with equations (3) and (5), where it can be seen that the proposed indicator depends on the product of healthy and current influence lines, which actually magnifies their differences. This effect is particularly evident for local damages near the supports in Figure 6(a). Furthermore, the sign of E_{BWIM} changes for different damage locations and thus this might give an indication of where the local damage has occurred. For instance, underestimations of axle weights (negative E_{BWIM}) by the B-WIM mid-span sensor indicate that the damage is near mid-span, whereas overestimations would imply a local damage near the supports. Combining the information of the three strain sensors it should be possible to roughly estimate the location of the damaged element.

The proposed indicator is able to detect local damages only in the case of statically indeterminate structures, such as fixed-fixed beams, structures with some rotational stiffness at the supports or multiple span continuous bridges. This is due to the fact that for the damage indicator to work there must a change in the structure's influence line. Hence, the indicator is not applicable to local stiffness reductions in a statically determinate structure where the influence line of strain will remain unaltered unless the sensor was located at the damaged location.

Numerical validation

In this section, Monte Carlo simulations are carried out to test the proposed SHM concept. Results are obtained for a beam with three structural conditions (healthy, with global and with local damages) traversed by two-axle vehicles with random properties described in the section on the simulation model. As before, simply supported and fixed-fixed cases are studied for the global damage case, whereas for the local damage only the indeterminate case can be analyzed. Additionally, the vehicles are simulated running over profiles ranging from class ‘A’ to ‘C’, which correspond to roads with well to average maintained pavements. These random profiles are generated based on the upper limit PSD defined in ISO 1995 for each particular class, i.e., geometric spatial means of $32 \cdot 10^{-6} \text{ m}^3$, $128 \cdot 10^{-6} \text{ m}^3$ and $512 \cdot 10^{-6} \text{ m}^3$ for classes ‘A’, ‘B’ and ‘C’ respectively.

The results are analyzed first for a healthy bridge with a class ‘A’ surface. Figure 7 shows the GVW prediction errors (E_{BWIM}) for 1000 vehicle crossing events with randomly generated properties following Table 3. The scatter in E_{BWIM} is significant and errors of $\pm 20\%$ are observed. The error variability is caused by the dynamic effects of the vehicle-bridge system that introduces deviations in both WIM systems (i.e., there is a considerable error in the estimations of $\{A\}$ and $\{\tilde{A}\}$ that are necessary to compute E_{BWIM} using equation (6)). In the case of the pavement-based WIM, the road profile nearby the weighing sensor causes the vehicle to oscillate producing variable reaction forces on the pavement that lead to some error in the estimation of the static weight. In the case of the B-WIM, the road profile and the vehicle-bridge interaction result in dynamic effects which introduce additional errors to the B-WIM estimates.

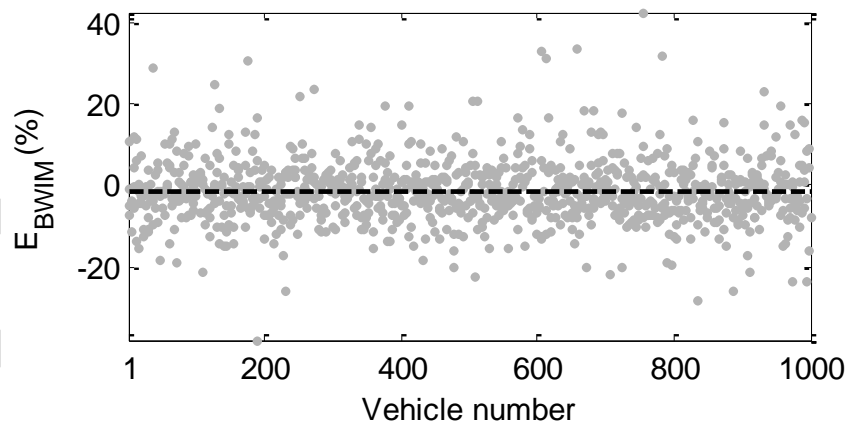


Figure 7. GVW prediction error for 1000 events on healthy beam (dots). Average E_{BWIM} (dashed line).

For the 1000 events presented in Figure 7, the pavement-based WIM system features relative errors in GVW of mean 1.96% and standard deviation 5.50. For the B-WIM system, the application of Moses’s algorithm to the strain records induced by each two-axle vehicle lead to relative errors in GVW of mean 1.42% and standard deviations 3.37. Following the European Standard on Weigh-In-Motion of Road Vehicles (European Standard 2010), both of these WIM systems are classified within the B(10) accuracy class according to the GVW criteria and C(15) according to the individual axle criteria. Even though the performance of both WIM systems is relatively poor in terms of accuracy forthcoming results will prove

them sufficient for SHM, once E_{BWIM} is averaged over a sample of vehicles high enough to compensate for the dispersion in individual results.

Figure 7 also shows the average E_{BWIM} which will be used in subsequent sections as an indicator of the structural health. In this case, the average E_{BWIM} is not zero, but 1.99%. This is due to the particular road profile of the site and unavoidable inaccuracies in weight estimations by both WIM systems (i.e., mean relative errors of 1.96% and 1.42% by pavement-based WIM and B-WIM respectively). On average, rougher profiles will induce larger dynamic oscillations of the vehicle and the bridge, and different profiles will produce different average E_{BWIM} values, however, it will be shown that these WIM errors do not affect the proposed assessment methodology significantly.

Global damage

Figure 8 shows the average daily E_{BWIM} results using the mid-span location for B-WIM, various degrees of global damage (= global reductions in stiffness) and three road conditions. The first 25 days are simulated on the assumption of a healthy structure. For every day, 1000 two-axle trucks are considered and only the daily average E_{BWIM} is shown in the figure. After those initial 25 days, the degree of global damage is increased by 10% every 25 days until a maximum of 30% damage introduced at the 75th day. 25-day average E_{BWIM} values of 3.11%, 14.89%, 28.72% and 47.37% are obtained in the presence of a class 'A' road profile for healthy, and 10%, 20% and 30% stiffness reductions respectively. These variations are in accordance with the results presented in Figure 4 where, for instance, a 20% stiffness reduction (occurring between day 50 and 75 in Figure 8) produced a B-WIM estimation of GVW with an average error of 25%. In Figure 8, daily average E_{BWIM} 's oscillate around an average monthly E_{BWIM} within a specific damage level. For a higher damage level, daily average E_{BWIM} 's are consistently higher than the average monthly E_{BWIM} in a healthier state. Sudden changes in daily average E_{BWIM} that remained consistent would clearly indicate that a global damage has occurred. Note that for global damage the same percentage variations are observed in each sensor of the B-WIM system. However, independent analysis of the average E_{BWIM} for each sensor makes the assessment of the structure's health more robust in case that one sensor gave dubious results or stopped working.

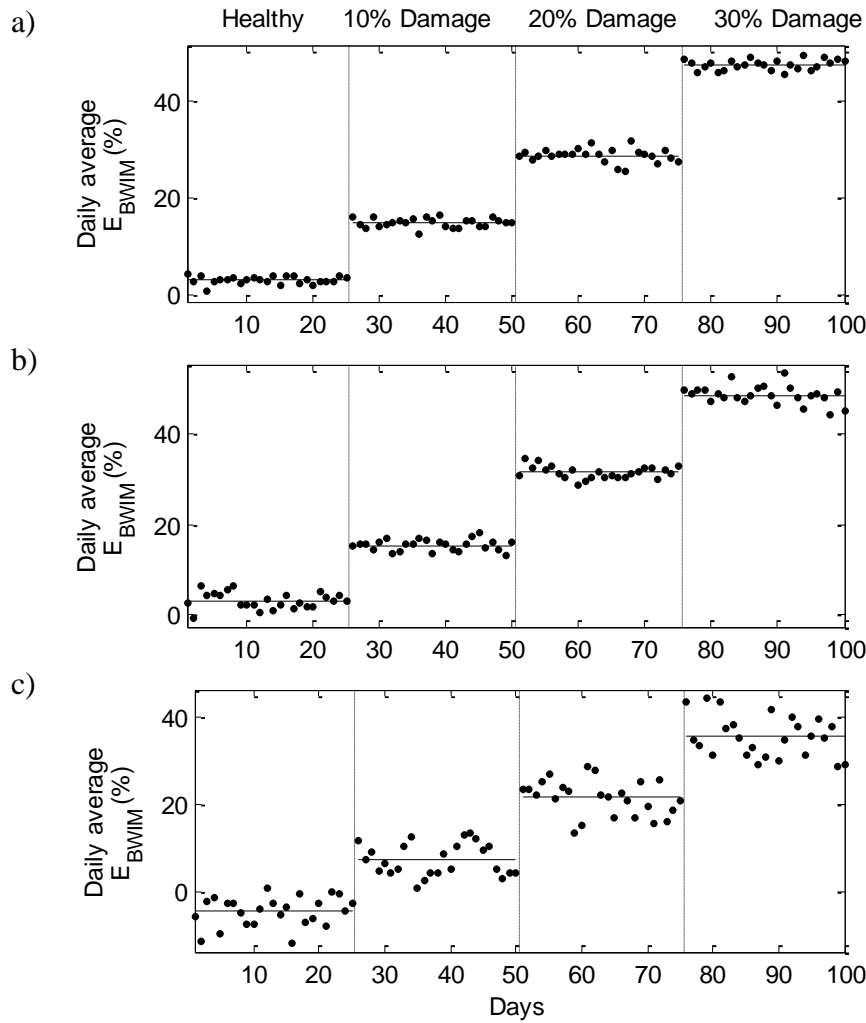


Figure 8. Daily average E_{BWIM} (dots) and 25-day average E_{BWIM} (solid straight lines) for different damage levels and road profiles: (a) class ‘A’, (b) class ‘B’, (c) class ‘C’.

The changes in the error of GVW estimates from one damage level to another level with a more severe 10% increase in stiffness loss, are relatively insensitive to the rougher ‘B’ and ‘C’ profiles. Obviously, rougher road profiles induce higher dynamic effects overall which results in a greater dispersion of individual E_{BWIM} estimations, but the latter does not significantly alter the average result and similar trends as in Figure 8(a) (class ‘A’) are observed for road profiles classified as ‘B’ and ‘C’ (ISO 1995) in Figures 8(b) and (c) respectively. So, 25-day average E_{BWIM} values of 3.22%, 15.45%, 31.50% and 48.61% are obtained for healthy, and 10%, 20% and 30% stiffness reductions respectively of a bridge with a class ‘B’ profile. Similarly, 25-day average E_{BWIM} values of -4.58%, 7.37%, 21.62% and 35.68% are obtained for healthy, and 10%, 20% and 30% stiffness reductions respectively of a bridge with a class ‘C’ profile. From these values it can be seen that changes in road profile class only affect changes in E_{BWIM} with damage severity slightly. Regarding the boundary condition of the bridge, the same relative variations of average E_{BWIM} with global damage are found for simply supported or fixed-fixed conditions.

Local damage

As discussed in Section on the comparison of WIM-based and frequency-based SHM approaches, local damage leads to different estimation errors by each sensor (Figure 6(a)),

with some sensor locations being insensitive to specific damage locations. Thus, the information of all sensors needs to be analyzed simultaneously. For this reason, Figure 9 presents the daily average E_{BWIM} for the three sensor locations under investigation for randomly generated vehicles on Class ‘A’ profile. A local damage 0.1 m long is introduced at $L/8$ and the severity of damage is increased by a sudden 25% stiffness loss every 25 days until a maximum damage of 75% is reached at the 75th day. Significant relative changes of E_{BWIM} are clear for sensors at $1/4L$ and $1/2L$. However, the sensor located at $3/4L$ gives no indication of any damage (in agreement with Figure 6(a)). For a 50% local damage at $L/8$, the expected changes in E_{BWIM} according to Figure 6(a) are 1.19%, 0.65% and -0.05% for sensors at $1/4L$, $1/2L$ and $3/4L$ respectively, which roughly correspond to the same values observed in Figure 9. For instance, in Figure 9(b) corresponding to $1/2L$, the 25-day average E_{BWIM} for the healthy and 50% stiffness reduction cases are -3.25% and -2.58% respectively which gives a relative change of 0.67%.

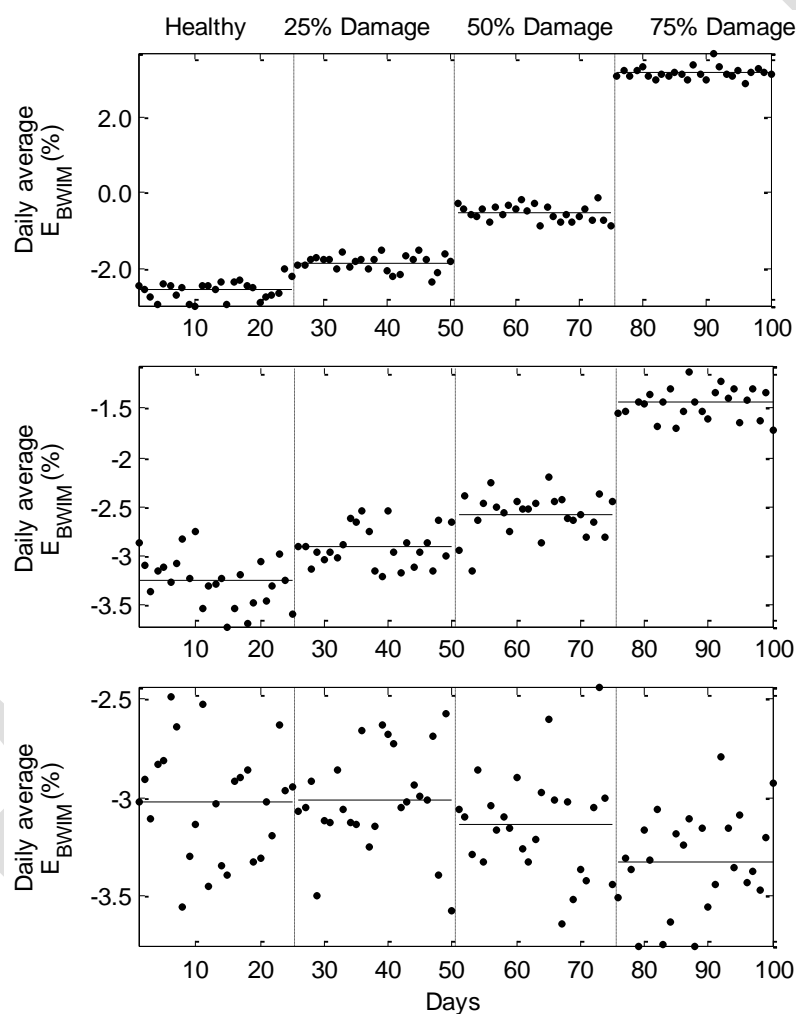


Figure 9. Daily average E_{BWIM} (dots) and 25-day average E_{BWIM} (solid straight lines) considering a local damage at $L/8$ for three B-WIM sensor locations (a) $1/4L$ (b) $1/2L$ (c) $3/4L$.

As expected, the relative variations of E_{BWIM} due to local damage are smaller than for global damage, although a stiffness loss is still identifiable. When a sudden change in error is observed in any of the strain sensors a careful investigation of the information should be performed. Furthermore, it is possible to roughly estimate the location of the damage. To prove this point, Monte Carlo simulations have been performed for seven bridges with seven different local damage locations (each representing a 50% stiffness loss along 0.1 m). Figure

10 shows the average monthly E_{BWIM} for 25000 events per damage location, assuming that there are 25 days of recorded data and 1000 events per day. As a result of averaging larger sets of data, more stable results and a resemblance can be found with the pattern in Figure 6(a) when road profile had not yet been considered. Figure 10 clearly shows that the E_{BWIM} is different for each sensor location and how this information can be used to identify the presence and the location of a local damage. The results presented in Figure 10 are more significant than those in Figure 6(a) (based on ideal WIM inputs) since now they include errors in the calculation of E_{BWIM} derived from a variety of dynamic effects such as vehicle-road and vehicle-bridge interactions, and variable vehicle's mechanical properties that will affect the accuracy of the WIM systems.

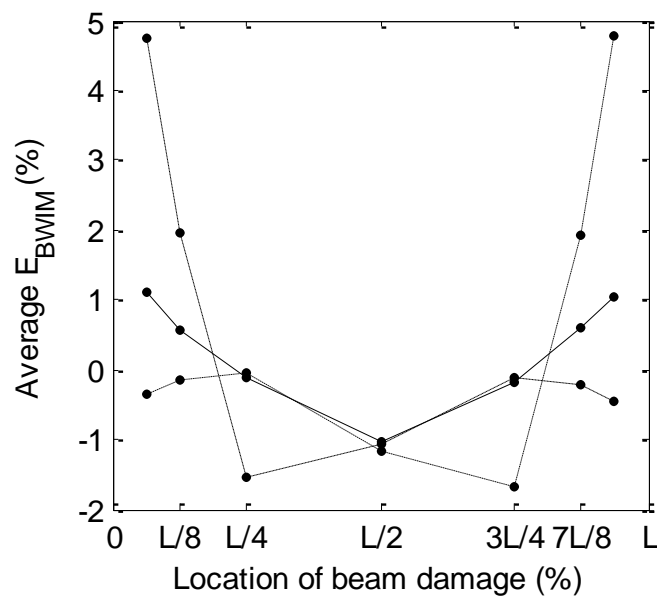


Figure 10. One month average E_{BWIM} for sensor located at $\frac{1}{4}L$ (dashed); $\frac{1}{2}L$ (solid); $\frac{3}{4}L$ (dash-dot) and a 50% local damage at seven different locations (dots).

Influence of noise

The results presented in previous sections considered uncorrupted responses (i.e., noise-free theoretical signals). However, in real WIM installations the presence of noise will affect their accuracy. Table 4 presents the mean (μ) and standard deviation (σ) of both WIM errors when estimating GVW and the E_{BWIM} indicator for the same 1000 events as presented in Figure 7 and various levels of noise. Here noise has been added as normally distributed random values proportional to the signal's magnitude, and its equivalent Signal to Noise Ratio (SNR) is shown in Table 4 for the case of a healthy scenario.

Table 4. Influence of signal noise on WIM, B-WIM and E_{BWIM}

Added random noise (%)	Equivalent SNR	GVW error by WIM (%)		GVW error by B-WIM (%)		E_{BWIM} (%)	
		μ	σ	μ	σ	μ	σ
0	$+\infty$	1.96	5.5	1.42	3.37	1.99	7.82
5	16.21	1.91	6.66	1.42	3.38	1.94	8.58
10	8.11	2.02	8.96	1.40	3.39	2.07	10.41
15	5.44	2.36	12.27	1.41	3.56	2.42	13.44
20	4.06	2.08	14.44	1.36	3.66	2.19	15.21

As expected the performance of the pavement-based WIM is affected significantly by noise and it shows greater dispersion in results than B-WIM for higher levels of noise. The short duration of the measurement by a WIM system prevents a safe removal of noise. However, a B-WIM system is only affected slightly by noise because GVW is calculated by effectively fitting a static response to a relatively long record of strain signal (duration given by the time the vehicle is on the bridge) which reduces the influence of the high frequency content induced by noise (i.e., it removes noise in a similar fashion to the removal of the dynamic component in the measured strain $\{\varepsilon^m\}$ by equation (3)). It is also noticeable that the average values of both WIM systems show only some small random variation due to noise. Therefore, even though E_{BWIM} presents a bigger dispersion (σ) in values for increasing noise levels, the mean E_{BWIM} remains fairly constant with noise compared to the noise-free scenario (1.99%). Since the proposed methodology proposes the use of average daily E_{BWIM} the influence of noise is limited and the presented conclusions still apply.

Discussion

The results presented here provide a proof of concept for a level 1 damage detection methodology that adds value to existing or planned WIM stations (originally applied to design and assessment of pavements and bridges, road and traffic management, and enforcement and road pricing) in a road network by making use of their output (namely, information on traffic weights and configuration) to monitor the bridges in the network. Some of the strengths of the proposed method are: (a) robustness, which increases with time and number of events, and is only affected slightly by the road profile and noise; (b) simplicity, since it does not require heavily instrumented bridges or the development of detailed computer models, (c) improved performance over frequency based level 1 methods and (d) cost-efficient exploitation of the multi-purpose data that WIM stations generate. Even though some successful B-WIM installations have been reported on wide orthotropic decks and long spans, it is acknowledged that the range of applicability of the method is limited by the current B-WIM technology that works best in short to medium span bridges carrying one or two lanes of traffic.

The reader might find that the planar numerical model used to validate the concept is relatively simple compared to reality. It is important to note that most of currently installed B-WIM systems do exactly the same calculations as presented here, reducing the problem to a 2D one. The transverse location of a vehicle within a lane is generally not considered to introduce significant errors on the weight estimates of a particular single traffic event. B-WIM systems based on Moses' algorithm generally place a few mechanical strain amplifiers across the instrumented section that are added together in order to compensate for small lateral variations of the vehicle within the lane. Therefore, the transverse effect is further reduced when considering the average results of a large population of events given that it can be safely assumed that, on average, there will be a dominant transverse location. If the latter was not the case, the B-WIM system will not be as accurate, but the damage indicator will still be operative as it depends on the relative inaccuracies between B-WIM and WIM systems as opposed to absolute values. If the relative inaccuracies between both systems change, it can denote a variation in the distribution of stiffness throughout the structure, except for temperature changes or sensor failure. Finally, the accuracies assumed for the theoretical WIM systems tested in this paper (i.e., a conservative accuracy class C(15) in the case of noise-free data) can be improved in practice when installed in road sites class I defined by a limiting criteria in rutting, deflection and evenness (European Standard 2010).

An accuracy class B(10) and better are not rare on smooth profiles in the case of estimation of GVW using short span stiff bridges (McNulty and OBrien 2003, González 2010) and multiple-sensor WIM systems (González 2010, Han et al 2012). In this paper, E_{BWIM} has been theoretically tested based on an average daily sample consisting of 1000 two-axle trucks. Clearly, the period of time or size of the population needed to calculate an average E_{BWIM} must be adjusted to specific site conditions such as identifiable number of trucks per day, characteristics of road, vehicles and bridges, noise and accuracy of both WIM systems.

Conclusions

This paper has introduced a new application of WIM technology to SHM of short to medium span highway bridges. It requires the information of weight estimations by two WIM systems: pavement-based and bridge-based. It has been shown that the relative difference in GVW estimation by both systems is a good indicator of the structure's condition. The use of this indicator at different bridge locations has allowed distinguishing between global and local damages, and it has even made possible to roughly estimate the location of damage. Furthermore, in both global and local damage situations, it has been shown that the proposed E_{BWIM} indicator has greater sensitivity to the occurrence of damage than a traditional level I damage identification technique based on tracking frequency changes. It is expected the findings in this paper will open a new range of possibilities to WIM technology.

Reference

- Cantero, D., González, A. and OBrien, E.J. (2011). "Comparison of bridge dynamic amplification due to articulated 5-axle trucks and large cranes." *Baltic Journal of Road and Bridge Engineering*, 6, 39-47.
- Doebling, S. W., Farrar, C. R. and Prime, M.B. (1998). "A summary review of vibration-based damage identification methods." *The Shock and Vibration Digest*, 30, 91-105.
- European Standard, Version 2010/4. Weigh-in-Motion of Road Vehicles.
- Gomez, H. C., Fanning, P.J., Feng, M. Q. and Lee S. (2011). "Testing and long-term monitoring of a curved concrete box girder bridge." *Engineering Structures*, 33, 2861–2869.
- González, A. (2010). "Development of a Bridge Weigh-In-Motion System." LAP Lambert Academic Publishing AG & Co, Germany.
- Han, L.D. Ko, S.S., Gu, Z. and Jeong, M.K. (2012). "Adaptive Weigh-in-Motion Algorithms for Truck Weight Enforcement." *Transportation Research Part C – Emerging Technologies*, 24(1), 256-269.
- ISO (1995). "Mechanical vibration – Road surface profiles - Reporting of measure data." International Organization for Standardization, ISO 8608:1995 (BS 7853:1996).
- McNulty, P. and OBrien, E.J. (2003). "Testing of bridge weigh-in-motion system in a sub-Arctic climate." *ASME Journal of Testing and Evaluation*, 31, 497-506.
- Moses, F. (1979). "Weigh-In-Motion system using instrumented bridges." *ASCE Transportation Engineering Journal*, 105, 233-249.

O'Brien, E.J., Quilligan, M.J. and Karoumi, R. (2006). "Calculating an influence line from direct measurements." *Bridge Engineering, Proceedings of the Institution of Civil Engineers*, 159, 31-34.

O'Brien, E.J., Žnidarič, A. and Ojio, T. (2008). "Bridge weigh-in-motion, latest developments and applications world wide". *Proc., International Conference on Heavy Vehicles*, Paris, France, 39-56.

O'Connor, A. and O'Brien E.J. (2005). "Traffic load modelling and factors influencing the accuracy of predicted extremes." *Canadian Journal of Civil Engineering*, 32(1), 270-278.

Wang, T.L., Liu, C., Huang, D. and Shahawy M. (2005). "Truck loading and fatigue damage analysis for girder bridges based on weigh-in-motion data." *ASCE Journal of Bridge Engineering*, 10, 12–20.

Wilson, S.P., Harris, N.K. and O'Brien, E.J. (2006). "The Use of Bayesian Statistics to predict Patterns of Spatial Repeatability." *Transportation Research Part C: Emerging Technologies*, 14(5), 303-315.

Yang, B. (2005). "Stress, Strain and Structural Dynamics." Elsevier Academic Press.

Žnidarič, A., Lavrič, I. and Kalin, J. (2008). "Measurements of Bridge Dynamics with a Bridge Weigh-In-Motion System". *Proc., International Conference on Heavy Vehicles*, Paris, France, 388-397.